Magazine of Civil Engineering

ISSN 2712-8172

journal homepage: http://engstroy.spbstu.ru/

DOI: 10.34910/MCE.106.14

Performance of composite connections strengthened with CFRP laminate

M. Ramezani ,
University of Alabama at Birmingham, Birmingham, Alabama, USA
E-mail: mramezani@uab.edu

Keywords: finite element method, reinforced concrete, stiffness, bending strength, fiber reinforced plastics, composite materials, retrofitting

Abstract. This paper presents the development of a three-dimensional non-linear finite element model to predict the moment-rotational response of partial depth endplate composite connections. A parametric study is performed to evaluate the influence of utilizing various sizes (i.e., length, width, and thickness) of external Carbon Fiber Reinforced Polymer (CFRP) laminates on the composite connection performance. The numerical analysis reveals that the flexural resistance of the retrofitted CFRP strengthened composite connection increases by up to around 20% and the rotation capacity decreases by approximately 60%. Moreover, the results indicate that applying CFRP laminate to the tension face of the composite slab can reduce the amount of rebar needed for the bending capacity of steel-concrete composite beam-to-column connections.

1. Introduction

Steel and concrete are the two widely used building materials in the construction industry [1], [2]. Each of these materials imparts certain strengths and weaknesses. For example, concrete exhibits low tensile strength and fracture toughness resulting in cracking [3], [4]. Structural steel elements, on the other side, are susceptible to buckling and exhibits poor fire resistance performance. The undesirable properties of these materials can be neutralized when they are combined to form a composite structure. The composite connection may be perceived as the addition of a reinforced concrete slab to the bare steel connection by providing an appropriate mechanism of shear transfer in between the concrete slab and the steel beams [5]. This mechanism is provided using shear studs that are welded to the top flange of the steel beam and embedded in concrete in order to act as a single unit. The key characteristics of composite connections (i.e., moment capacity, rotation capacity and rotational stiffness) are considerably affected by many factors such as joint type, slab depth, reinforcement bar ratio, the degree of shear interaction and load application procedure [6]–[14].

In addition, to maintain the favorable performance of composite connections during their service life, the flawless performance of the steel and concrete components should be continuously provided. In this regard, steel and concrete need special modification and rehabilitation schemes to withstand their primary properties for a long period of time when exposed to service environments. As for instance, it is estimated that developed countries assign approximately 40% of their total construction industry budget for repair and maintenance purposes of the existing infrastructures [15]. In case of a reinforced concrete (RC) structures, the main detrimental factors are the increase in applied loads, corrosion of steel reinforcing bars and unexpected events such as earthquakes. The retrofit of RC elements can be achieved by adding steel or Fiber Reinforced Polymer (FRP) materials including rods [16], [17], plates [18] and innovative systems [19] to the damaged RC element. In the case of retrofitting plates, steel or FRP plates are attached to the surface of the concrete element in such a way that the slip between the connected materials is prevented and they act compositely in carrying the load. The FRP materials are more attractive than steel, primarily due to higher strength-to-weight ratio, resistance to many chemicals and metal-corrosive agents as well as easier

Ramezani, M. Performance of composite connections strengthened with CFRP laminate. Magazine of Civil Engineering. 2021. 106(6). Article No. 10614. DOI: 10.34910/MCE.106.14

handling and installation. Thus, external bonding of FRP plates has become a widely popular method for the strengthening of different RC structural members such as beams, columns and slabs [20], [21].

An abundance of tests over the last two decades have shown that the bending capacity of flexural members such as RC beams and slabs to be enhanced by applying FRP overlays to their tension face [22], [23]. Parvin and Granata [24], Mosallam [25] and Gergely et al. [26] carried out experimental and numerical studies on the behavior of RC joints strengthened with FRP laminates. The authors reported the increase in the flexural capacity and decrease in the ultimate rotation of joints as a result of FRP strengthening of RC connections. Esfahani et al. [27] and Almusallam et al. [28] examined the effect of reinforcement bar ratio on the behavior of beams strengthened with FRP laminates. They pointed out the enhancement in bending capacity and stiffness of the retrofitted beams. On the other hand, a significant absence of literature exists on the behavior of endplate composite connections strengthened with FRP laminates.

The main objective of this study is to evaluate the moment-rotational response of endplate composite connections including strengthening of the slab using different sizes and thickness of Carbon Fiber Reinforced Polymer (CFRP) laminates attached to the tension face of the slab. To this end, a three dimensional (3D) non-linear finite element model is developed in ANSYS software to perform a parametric study. In addition, various values of reinforcement bar ratio in the slab is considered to investigate the possibility of decreasing the rebar in the presence of the CFRP laminate. This will reduce rebar congestion in the composite joint resulting in cost and time savings in rehabilitation projects.

2. Methods

The Finite Element Method (FEM) is a numerical technique that can be used to solve complicated problems in engineering by breaking down a complex problem into a large number of simple problems. In this section, a short description of the experimental program that was used as the calibration basis for the numerical studies is initially presented. The finite element models are then used in parametric analyses of partial depth endplate composite connections.

The specimen SCJ10 tested by Xiao [13], [14] at The University of Nottingham serves as the base model (un-strengthened model) to compare with those finite element models strengthened with CFRP laminates. The specimen SCJ10 is depicted in Figure 1. Two 305×165×UB40 (beam element) of 1.6 m in length and one 203×203×UC52 (column element) of 1.2 m in height are connected to form the cruciform configuration. The beams are connected to the column flanges at a height of 500 mm by means of partial-depth endplates (190×150×10 mm) welded to the steel beam and bolted to the column flange with two rows of M20 Grade 8.8 bolts. A 120 mm deep slab with RMF CF46 profiled metal decking is used. The slab rebar ratio is 0.8%. Two point loads of the same magnitude are applied symmetrically to each cantilever at 1.5 m from the column flange.

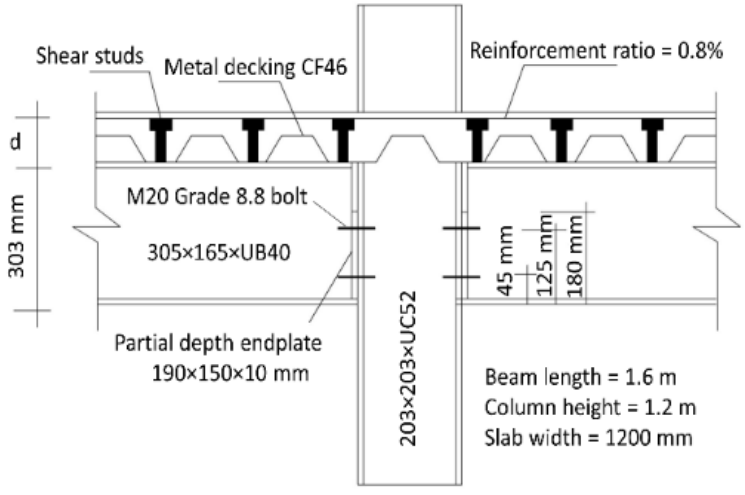

Figure 1. Cruciform arrangement of partial depth endplate composite connection (SCJ10).

In this study, the advantage of the symmetry is used to model the composite connections in order to reduce the problem size. Therefore, it is essential to address the problem with proper boundary conditions. To define the support condition or to establish symmetry, appropriate restraints on nodes or node sets are required. Regarding symmetry about two axes of the cross-section, the concrete-steel composite connections are modeled with half-length (see Figure 2). All nodes on the line of symmetry are restrained against both translation and rotation in the *z*-axis direction.

The metal deck and beams are modeled with eight-node thin shell elements (SHELL281) and the concrete slab is modeled using a solid element (SOLID185). The SOLID185 element has eight nodes with three degrees of freedom at each node. The element has plasticity, hyper-elasticity, stress stiffening, creep, large deflection and large strain capabilities. The reinforcement bars are modeled using the link element (LINK8) and shear studs are idealized by twenty-node solid elements (SOLID95). The eight-node solid elements (SOLID45) is used to model the column, endplate and bolts.

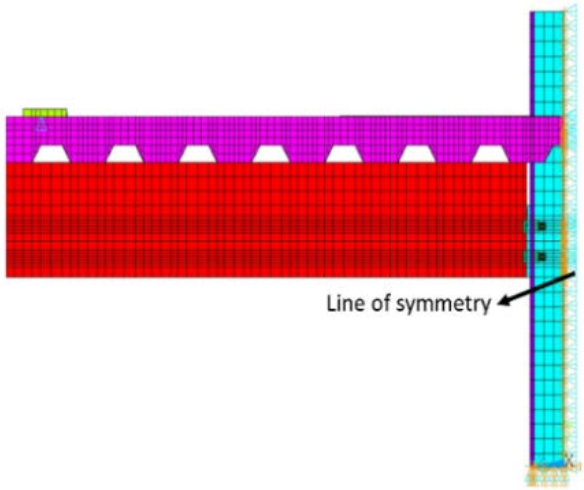

Figure 2. Typical finite element model with Boundary conditions.

The interaction between the metal deck and steel beams is not fully bonded. Thus, surface-to-surface contact elements are used as the interface element between the metal deck and the steel beam to prevent any penetration of steel decking into the steel beam. To model this behavior, the surface-to-surface contact elements, CONTA174 and TARGE170 are superimposed on the surface of the solid or shell elements which form the interface. Each of these "contact pairs" is also capable of representing the slide between the two surfaces activated by defining a friction coefficient. The surface-to-surface contact model also defines the complex interfaces between the endplate and the column flange, the shear studs and concrete as well as the column flange and concrete. The coefficient of friction is assumed equal to 0.45 in this research.

For the material properties, ANSYS requires input of the modulus of elasticity, yield stress and Poisson's ratio. In this study, Poisson's ratio values of 0.3 and 0.2 are used for steel and concrete, respectively. The relationship between the compressive strength of concrete and its tensile strength and modulus of elasticity is expressed as shown in Equations (1) and (2), respectively [29]:

$$f_r = 0.632\sqrt{f_c^{'}} \tag{1}$$

$$E_c = 4700\sqrt{f_c^{'}} \tag{2}$$

where f_r, $f_c^{'}$ and E_c are the tensile strength, compressive strength and modulus of elasticity of concrete, respectively. The compressive uniaxial stress-strain relationship for concrete in the ascending branch to compute the multi-linear isotropic stress-strain curve is calculated using Equations (3) to (5) [30]:

$$f = \frac{E_c \varepsilon}{1+\left(\frac{\varepsilon}{\varepsilon_0}\right)^2} \tag{3}$$

$$\varepsilon_0 = 2\frac{f_c^{'}}{E_c} \tag{4}$$

$$E_c = \frac{f}{\varepsilon} \tag{5}$$

where ε is the strain, f is the stress at any strain and ε_0 is the strain at the ultimate compressive strength. The stress-strain behavior adopted for concrete is shown in Figure 3.

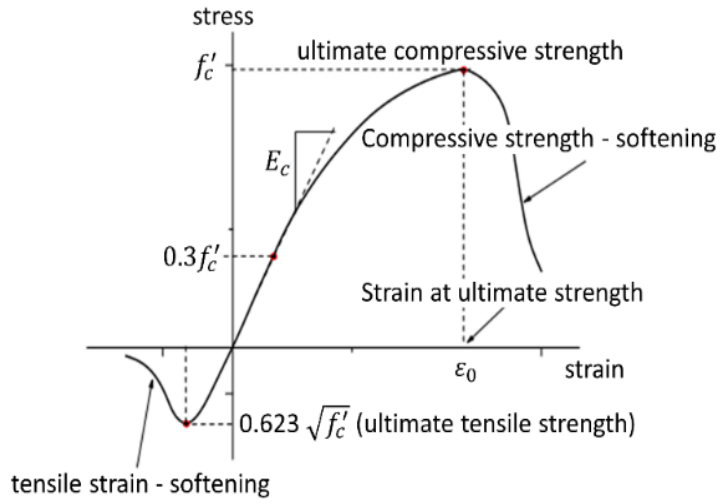

Figure 3. Uniaxial stress-strain curve adopted for concrete.

The shear studs and metal deck are modeled using a bilinear stress-strain curve with the bilinear isotropic hardening option (BISO). The bilinear stress-strain curve is capable of representing elastic-perfectly plastic material behavior with equal yield stresses in tension and compression as well as with the hardening option.

The steel reinforcement is modeled for nonlinear analysis as an elastic-plastic material using a three linear stress-strain law symmetrical is tension and compression (see Figure 4 (a)). An increase of deformation over the elastic limit leads to the exhibition of a yielding plateau phase. After the perfectly plastic branch, strain-hardening behavior initiates. The plastic strain deformation at the end of the yielding plateau (ε_{st}) and the modulus of elasticity in the hardening phase (E_{st}) for steel reinforcement bars are obtained using Equations (6) and (7), respectively [31], [32]:

$$\varepsilon_{st} = 3\varepsilon_{sy} \tag{6}$$

$$E_{st} = 0.02E_y \tag{7}$$

where ε_{sy} and E_y are the yield strain and the modulus of elasticity, respectively.

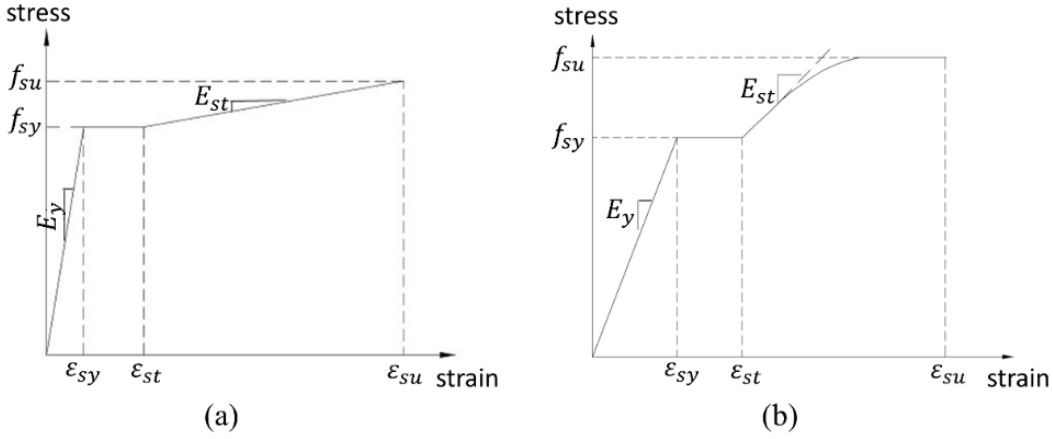

Figure 4. Stress-strain curve for (a) steel reinforcement bars (b) beam, column, bolts and steel deck.

In line with Gattesco [33], other structural steel parts are modeled using a stress-strain relationship that incorporates multi-linear isotropic hardening (see Figure 4 (b)). Amadio and Fragiacomo [32] have proposed Equations (8) and (9) for the plastic strain deformation at the end of ε_{st} and E_{st}, respectively.

$$\varepsilon_{st} = 15\varepsilon_{sy} \tag{8}$$

$$E_{st} = 0.015E_y \tag{9}$$

In this research, a 3-D layered structural element (SOLID46) with three degrees of freedom at each node is used to model the CFRP laminates. The element allows up to 250 layers and translation in the *x,*

y, and *z* directions. The element is defined by eight nodes, layer thickness, layer material direction angles and orthotropic material properties. This study assumes that the strength of the epoxy used to attach the CFRP laminates to the surface of concrete was sufficiently high to support the full bonded assumption. In line with similar studies [34], [35], the CFRP laminate "MBRACE® laminate 460/1500" with a 71% volume fraction of carbon fiber is adopted for this research. The material properties of the CFRP material are given in Table 1.

Table 1. Material properties of CFRP laminate.

CFRP laminate	Tensile modulus (GPa)	Poisson's ratio	Tensile strength (MPa)	Elongation at break (%)	Thickness (mm)
MBRACE ® LAMINATE 460/1500	478.730	0.36	1607	0.36	1.45

3. Results and Discussion

In this section, the moment-rotation curves are plotted using the obtained numerical results. From this curve, the ultimate moment and rotation capacities are determined and compared with the existing experimental test data [13], [14] in order to validate the finite element results. Then, a direct comparison between the strengthened and un-strengthened composite connections are made and the effect of implementing CFRP external reinforcing laminates is studied.

3.1. Model validation

The experimental and numerical moment-rotation curves for the un-strengthened specimen (SCJ10) are compared in Figure 5. The experimental values of ultimate moment and rotation capacities were 147.8 kN.m and 16.5 mRad, respectively [13], [14]. The ultimate moment and rotation capacities obtained from FEM model for SCJ10 are 146.5 kN.m and 16.1 mRad, respectively, which are very close to the experimental test data. Note that both the experimental and FEM curves follow a similar trend. In the initial phase, the connection behaves linearly which is then followed by nonlinear behavior where the connection gradually loses its rotational stiffness as rotation increases.

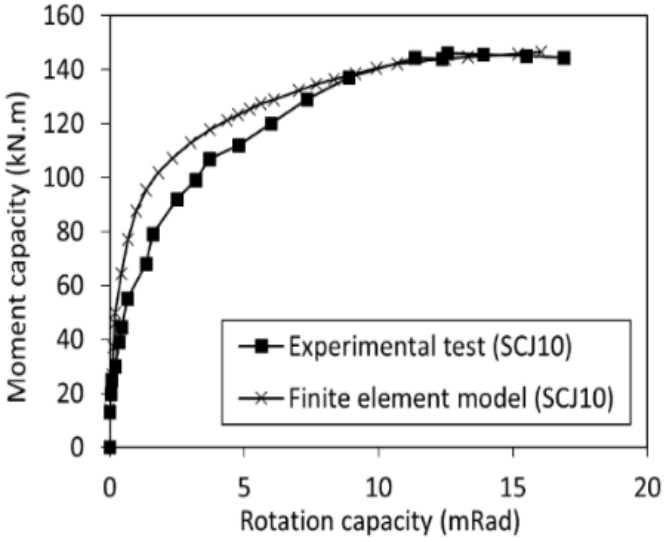

Figure 5. Comparisons between experimental and FEM results.

Also, The failure mode for SCJ10 using FEM shows good correlation with the experimental test results [13]; both experimental and FEM models failed due to the column web buckling (see Figure 6 (a) and 6 (b)). The deformation of the partial depth endplate due to the applied load can also be seen in Figure 6 (c). These confirm the accuracy of the developed finite element model.

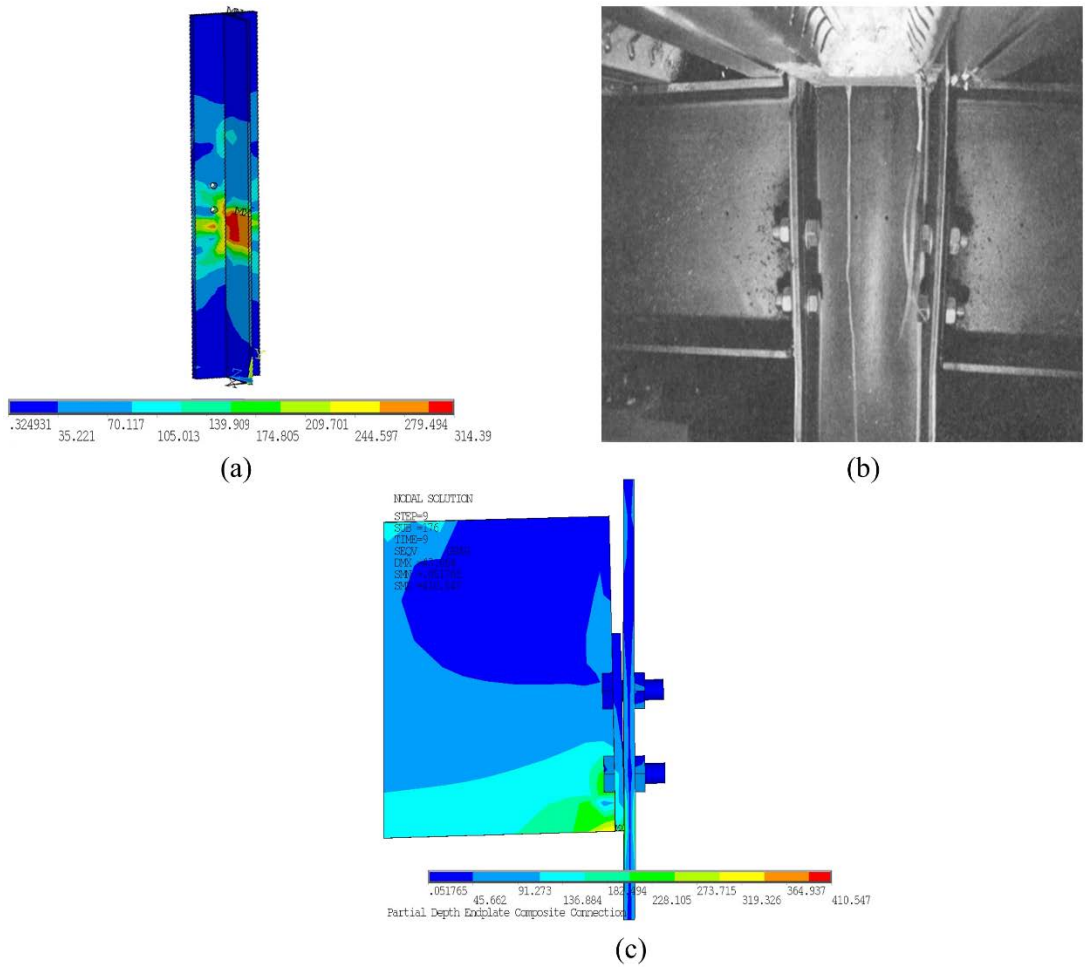

Figure 6. (a) FEM failure mode (b) experimental failure mode (c) deformation of partial depth endplate after FE simulation.

3.2. Parametric study

3.2.1. Effect of CFRP length and width

To investigate the effect of the CFRP laminate dimensions, five models with different widths and lengths are developed. Table 2 shows the configurations of these models. A composite connection without a CFRP laminate is analyzed to serve as a reference model to comparison with those models reinforced with CFRP laminates. In this research, the CFRP laminate have width values between 30% and 60% of the slab width. The length of the CFRP laminate is varied from 20% to 40% of the length of the composite slab. The thickness of the laminates is 1.45 mm.

Table 2. CFRP laminate dimensions.

Test ID	CFRP laminate configuration		
	Width (%slab width)	Length (%slab length)	Thickness (mm)
CFRP W30×L30	30	30	1.45
CFRP W45×L30	45		
CFRP W50×L20	50	20	
CFRP W60×L30	60	30	
CFRP W60×L40		40	

Figure 7 shows a typical FE model of a CFRP laminate applied to the tension face of the partial depth endplate composite connection. A finer mesh is used around the shear studs due to the stress concentration in their vicinities.

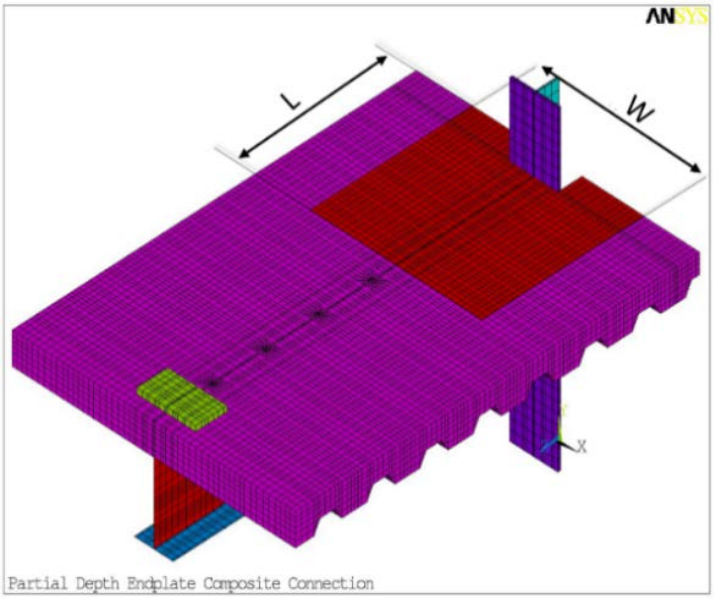

Figure 7. Typical FE model of a composite connection strengthened with CFRP laminate.

The ultimate moments and rotation capacities for un-strengthened and strengthened models with different CFRP laminate configurations is shown in Table 3. Also, the moment-rotation curves for the FE models are presented in Figure 8. The results show that applying CFRP laminate to the tension face of the composite connection will increase the ultimate moment and rotational stiffness of the connection compared with the un-strengthened model. The rotation capacity of the CFRP strengthened connection is considerably lower than the un-strengthened specimen (SCJ10). Moreover, it is clear that the length of the CFRP laminate has greater influence on the moment capacity than its width. For example, the ultimate moment and rotation capacity for test ID CFRP W60×L40 is increased by 8.2% and 9.5% compared with CFRP W60×L30, respectively. In addition, test ID CFRP W50×L20 with the smallest length exhibits the smallest moment capacity amongst all the FE models.

Table 3. FEM results of partial depth composite connections with and without CFRP laminate.

Test ID	Ultimate Moment (kN.m)	Rotation capacity (mRad)
Un-strengthened model (SCJ10)	146.47	16.05
CFRP W30×L30	150.34	6.910
CFRP W45×L30	158.10	6.747
CFRP W50×L20	149.08	7.573
CFRP W60×L30	162.63	6.631
CFRP W60×L40	175.92	7.264

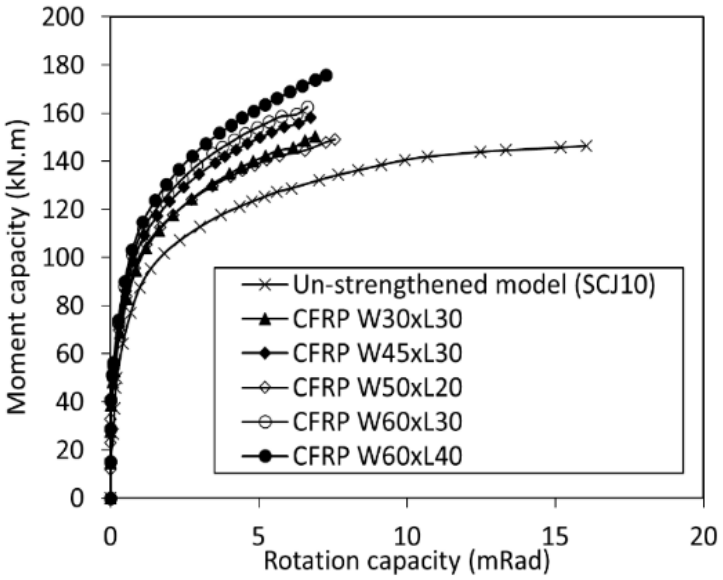

Figure 8. Moment-rotation curves for un-strengthened and strengthened models.

3.2.2. Effect of CFRP thickness

To investigate the effect of the CFRP laminate thickness on the moment-rotation curve of the composite connection, CFRP W60×L40 is modeled with different sheet thicknesses. Table 4 shows the configurations and moment/rotation capacities of the considered models. From the FE results, it can be seen that by increasing the thickness of CFRP sheets, the moment capacity of the composite connection is slightly increased. By increasing the CFRP laminate thickness from 2 mm to 5 mm, the moment and rotation capacities are increased by only 5.5% and 4.5%, respectively.

Table 4. FEM results of various configurations of CFRP reinforced composite connections.

Test ID	CFRP laminate configuration			Moment capacity (kN.m)	Rotation capacity (mRad)
	Width (%slab width)	Length (%slab length)	Thickness (mm)		
CFRP W60×L40	60	40	1.45	175.92	7.264
CFRP W60×L40×T2			2	176.16	6.378
CFRP W60×L40×T5			5	185.82	6.665

3.3. Effect of reinforcement bar ratio

To investigate the influence of the reinforcement bars on the composite connection, test IDs SCJ10×R0.2 and SCJ10×R0.4 with identical joint details but different areas of reinforcement bar from SCJ10 are considered. The reinforcement bar ratios for SCJ10×R0.2 and SCJ10×R0.4 are 0.2 % and 0.4 %, respectively. The results obtained from these finite element models are shown in Table 5. The FEM results indicate that by decreasing the reinforcement bar ratio, the moment capacity is decreased. The moment capacity of SCJ10×R0.4 and SCJ10×R0.2 reduces by 13.6 % and 22.2 %, respectively, compared with test ID SCJ10 (reinforcement bar ratio of 0.8%). However, the rotation capacity of SCJ10×R0.2 is slightly higher than SCJ10×R0.4 (5.8% higher).

As stated previously, one of the main objectives of this study is to investigate the feasibility of decreasing the reinforcing bars in the presence of CFRP laminate at the tension face of the composite connection. Two models of CFRP W60×L40×R0.2 and CFRP W60×L40×R0.4 are therefore considered. The specifications and moment/rotation capacities of these models are shown in Table 5. The moment capacity of test ID CFRP W60×L40×R0.2 is increased by 25.3 % and the rotation capacity is decreased by 64.5 % (rotational stiffness is increased) compared with test ID SCJ10×R0.2. Also, the moment capacity of test ID CFRP W60×L40×R0.4 is 18.5 % more than the moment capacity of its un-strengthened model (SCJ10×R0.4). From the FEA results, it is obvious that CFRP laminate can reduce the amount of reinforcement bars needed to provide the required bending strength of a composite connection.

Table 5. FEM results of various reinforcement bar ratios with and without CFRP laminate.

Test ID	CFRP laminate configuration			Moment capacity (kN.m)	Rotation capacity (mRad)
	Width (%slab width)	Length (% slab length)	Reinforcement bar ratio (%)		
SCJ10×R0.2	-	-	0.2	113.93	9.110
SCJ10×R0.4			0.4	126.60	8.612
SCJ10			0.8	146.47	16.05
CFRP W60×L40×R0.2	60	40	0.2	142.77	3.233
CFRP W60×L40×R0.4			0.4	149.97	3.688

4. Conclusions

The full scale testing of composite connections to obtain the mechanical properties such as the strength and stiffness requires expensive and time-consuming experiments. A straightforward alternative method is to use finite element analysis, yet the numerical results must be verified by available experimental data. In this paper, a three-dimensional nonlinear finite element analysis is carried out using ANSYS software to investigate the influence of various parameters on the moment-rotational response of partial depth endplate composite connections. The comparison between the experimental and finite element results proves that finite element analysis could precisely predict the complex behavior of composite connections. The following conclusions can be drawn:

- The results show that the application of CFRP laminate to the tension face of the slab leads to significant enhancements in flexural strength and stiffness of the partial depth endplate composite connections. Under identical loading conditions, applying external CFRP laminate exhibits 20.1% increase in the ultimate moment and 58.7% decrease in joint rotation, compared with the un-strengthened case.
- Increasing the CFRP laminate thickness can slightly improve the performance of composite beam-to-column connections by reducing the joint rotation and increasing the moment capacity. The increase in the CFRP laminate thickness from 2 to 5 mm results in a slight increase in the flexural strength of the composite connection.
- Applying CFRP laminate to the tension face of the slab can reduce the amount of reinforcement bars needed for flexural capacity of the composite beam-to-column connections by contributing to the tensile force. This will alleviate rebar congestion in the joint and make the whole structure more cost effective.

References

1. Bakis, C.E., Bank, L.C., Brown, Vl., Cosenza, E., Davalos, J.F., Lesko, J.J., Machida, A., Rizkalla, S.H., Triantafillou, T.C. Fiber-reinforced polymer composites for construction—State-of-the-art review. Journal of composites for construction. 2002. 6(2). Pp. 73–87. DOI: 10.1061/(ASCE)1090-0268(2002)6:2(73).
2. Ramezani, M. Design and predicting performance of carbon nanotube reinforced cementitious materials: mechanical properties and dipersion characteristics. Electronic Theses and Dissertations. Paper 3255. DOI: 10.18297/etd/3255.
3. Ramezani, M., Kim, Y.H., Sun, Z. Modeling the mechanical properties of cementitious materials containing CNTs. Cement and Concrete Composites. 2019. 104. Pp. 1–21 (103347). DOI:10.1016/j.cemconcomp.2019.103347.
4. Ramezani, M., Kim, Y.H., Sun, Z. Mechanical Properties of Carbon Nanotube Reinforced Cementitious Materials: Database and Statistical Analysis. Magazine of Concrete Research. 2019. Pp. 1–25. DOI: 10.1680/jmacr.19.00093.
5. Ramezani, M. Finite element model of composite connections strengthened with CFRP laminates. DOI: 10.31224/osf.io/sfkwv.
6. Ahmed, B., Nethercot, D.A. Prediction of initial stiffness and available rotation capacity of major axis composite flush endplate connections. Journal of Constructional Steel Research. 1997. 41(1). Pp. 31–60. DOI: 10.1016/S0143-974X(96)00053-3.
7. Anderson, D., Najafi, A.A. Performance of composite connections: Major axis end plate joints. Journal of Constructional Steel Research. 1994. 31(1). Pp. 31–57. DOI: 10.1016/0143-974X(94)90022-1.
8. Thai, H.T., Uy, B. Rotational stiffness and moment resistance of bolted endplate joints with hollow or CFST columns. Journal of Constructional Steel Research. 2016. 126. Pp. 139–152. DOI: 10.1016/j.jcsr.2016.07.005.
9. Song, Y., Uy, B., Wangb, J. Numerical analysis of stainless steel-concrete compositebeam-to-column joints with bolted flush endplates. Steel and Composite Structures. 2019. 33(1). Pp. 143–162. DOI: 10.12989/scs.2019.33.1.143.
10. Waqas, R., Uy, B., Thai, H.T. Experimental and numerical behaviour of blind bolted flush endplate composite connections. Journal of Constructional Steel Research. 2019. 153. Pp. 179–195. DOI: 10.1016/j.jcsr.2018.10.012.
11. Guo, L., Wang, J., Wang, W., Wang, C. Cyclic tests and analyses of extended endplate composite connections to CFDST columns. Journal of Constructional Steel Research. 2020. 167. Pp. 1–22 (105937). DOI: 10.1016/j.jcsr.2020.105937.
12. Davari, M., Ramezani, M., Hayatdavoodi, A., Nazari, M. Finite Element Analysis of Precast Concrete Connections under Incremental load. Australian Journal of Basic and Applied Sciences. 2012. 6(12). Pp. 341–350.
13. Xiao, Y., Choo, B.S., Nethercot, D.A. Composite connections in steel and concrete. I. Experimental behaviour of composite beam-Column connections. Journal of Constructional Steel Research. 1994. 31(1). Pp. 3–30. DOI: 10.1016/0143-974X(94)90021-3.
14. Xiao, Y., Choo, B.S., Nethercot, D.A. Composite connections in steel and concrete. Part 2—Moment capacity of end plate beam to column connections. Journal of Constructional Steel Research. 1996. 37(1). Pp. 63–90. DOI: 10.1016/0143-974X(95)00015-N.
15. Mehta, K., Monteiro, P. Concrete: Microstructure, Properties, and Materials. 3rd edn. McGraw-Hill Inc. New York, 2006.
16. Almassri, B., Al Mahmoud, F., Francois, R. Behaviour of corroded reinforced concrete beams repaired with NSM CFRP rods, experimental and finite element study. Composites Part B: Engineering. 2016. 92. Pp. 477–488. DOI: 10.1016/j.compositesb.2015.01.022.
17. Almassri, B., Barros, J.A.O., Al Mahmoud, F., Francois, R. A FEM-based model to study the behaviour of corroded RC beams shear-repaired by NSM CFRP rods technique. Composite Structures. 2015. 123. Pp. 204–215. DOI: 10.1016/j.compstruct.2014.12.043.
18. Napoli, A., Bank, L.C., Brown, V.L., Martinelli, E., Matta, F., Realfonzo, R. Analysis and design of RC structures strengthened with mechanically fastened FRP laminates: A review. Composites Part B: Engineering. 2013. 55. Pp. 386–399. DOI: 10.1016/j.compositesb.2013.06.038.
19. Mosallam, A., Elsanadedy, H.M., Almusallam, T.H., AL-Salloum, Y.A., Alsayed, S.H. Structural evaluation of reinforced concrete beams strengthened with innovative bolted/bonded advanced frp composites sandwich panels. Composite Structures. 2015. 124. Pp. 421–440. DOI: 10.1016/j.compstruct.2015.01.020.
20. Huang, L., Yan, B., Yan, L., Xu, Q., Tan, H., Kasal, B. Reinforced concrete beams strengthened with externally bonded natural flax FRP plates. Composites Part B: Engineering. 2016. 91. Pp. 569–578. DOI: 10.1016/j.compositesb.2016.02.014.
21. Yuan, X., Zhu, C., Zheng, W., Hu, J., Tang, B. Flexure Performance of Externally Bonded CFRP Plates-Strengthened Reinforced Concrete Members. Mathematical Problems in Engineering. 2020. 2020. Pp. 1–15. DOI: 10.1155/2020/2604024.
22. Banjara, N.K., Ramanjaneyulu, K. Investigations on behaviour of flexural deficient and CFRP strengthened reinforced concrete beams under static and fatigue loading. Construction and Building Materials. 2019. 201. Pp. 746–762. DOI: 10.1016/j.conbuildmat.2019.01.010.
23. Rashid, K., Li, X., Deng, J., Xie, Y., Wang, Y., Chen, S. Experimental and analytical study on the flexural performance of CFRP-strengthened RC beams at various pre-stressing levels. Composite Structures. 2019. 227. Pp. 1–12 (111323). DOI: 10.1016/j.compstruct.2019.111323.

24. Parvin, A., Granata, P. Investigation on the effects of fiber composites at concrete joints. Composites Part B: Engineering. 2000. 31(6–7). Pp. 499–509. DOI: 10.1016/S1359-8368(99)00046-3.
25. Mosallam, A.S. Strength and ductility of reinforced concrete moment frame connections strengthened with quasi-isotropic laminates. Composites Part B: Engineering. 2000. 31(6–7). Pp. 481–497. DOI: 10.1016/S1359-8368(99)00068-2.
26. Gergely, J., Pantelides, C.P., Reaveley, L.D. Shear strengthening of RCT-joints using CFRP composites. Journal of Composites for Construction. 2000. 4(2). Pp. 56–64. DOI: 10.1061/(ASCE)1090-0268(2000)4:2(56).
27. Esfahani, M.R., Kianoush, M.R., Tajari, A.R. Flexural behaviour of reinforced concrete beams strengthened by CFRP sheets. Engineering Structures. 2007. 29(10). Pp. 2428–2444. DOI: 10.1016/j.engstruct.2006.12.008.
28. Almusallam, T.H., Elsanadedy, H.M., Al-Salloum, Y.A. Effect of longitudinal steel ratio on behavior of RC beams strengthened with FRP composites: Experimental and FE study. Journal of Composites for Construction. 2015. 19(1). Pp. 1–18. DOI: 10.1061/(ASCE)CC.1943-5614.0000486.
29. ACI Committee 318. Building Code Requirements for Structural ConcreteDetroit, MI, 2014.
30. MacGregor, J.G., Wight, J.K. Reinforced concrete: mechanics and design. 3rd edn. Prentice Hall Inc. Upper Saddle River, New Jersey, 2009.
31. Gil, B., Bayo, E. An alternative design for internal and external semi-rigid composite joints. Part II: Finite element modelling and analytical study. Engineering Structures. 2008. 30(1). Pp. 232–246. DOI: 10.1016/j.engstruct.2007.03.010.
32. Amadio, C., Fragiacomo, M. Analysis of rigid and semi-rigid steel-concrete composite joints under monotonic loading - Part I: Finite element modelling and validation. Steel and Composite Structures. 2003. 3(5). Pp. 349–369. DOI: 10.12989/scs.2003.3.5.349.
33. Gattesco, N. Analytical modeling of nonlinear behavior of composite beams with deformable connection. Journal of Constructional Steel Research. 1999. 52(2). Pp. 195–218. DOI: 10.1016/S0143-974X(99)00026-7.
34. Wu, C., Zhao, X., Duan, W.H., Al-Mahaidi, R. Bond characteristics between ultra high modulus CFRP laminates and steel. Thin-Walled Structures. 2012. 51. Pp. 147–157. DOI: 10.1016/j.tws.2011.10.010.
35. Wu, C., Zhao, X.L., Chiu, W.K., Al-Mahaidi, R., Duan, W.H. Effect of fatigue loading on the bond behaviour between UHM CFRP plates and steel plates. Composites Part B: Engineering. 2013. 50. Pp. 344–353. DOI: 10.1016/j.compositesb.2013.02.040.

Contacts:

Mahyar Ramezani, mramezani@uab.edu